Magnetic properties of palladium-graphite multilayers

Masatsugu Suzuki* and Itsuko S. Suzuki
Department of Physics, State University of New York at Binghamton, Binghamton, New York 13902-6016

Jürgen Walter†
Osaka National Research Institute, AIST, MITI, 1-8-31, Midorigaoka, Ikeda, Osaka 563-8577, Japan
(Received 15 March 2000; revised manuscript received 12 June 2000)

dc magnetization and ac magnetic susceptibility of Pd graphite based on natural graphite have been measured using a superconducting quantum interference device magnetometer. In Pd-*G*, Pd multilayers are sandwiched between adjacent graphite layers. This sandwich structure is periodically stacked along the *c* axis. Pd layers are formed of Pd nanoparticles in the form of either a one-dimensional chain or two-dimensional platelets. There are two kinds of magnetic behavior depending on sample. Pd-$G(1)$ is an itinerant spin system with an antiferromagnetic ordered phase below $T_N(=3.8\,\mathrm{K})$. No spin-glass-like behavior occurs around T_N. Pd-$G(2)$ is a quasi-two-dimensional *XY*-like ferromagnet with very weak antiferromagnetic interplanar interaction. It undergoes two magnetic phase transitions at $T_{cu}(=14.2\pm0.2\,\mathrm{K})$ and $T_{cl}(=11\,\mathrm{K})$. Between T_{cu} and T_{cl}, a two-dimensional ferromagnetic spin order is established within nanoparticles in the Pd layers. Below T_{cl} there appears a three-dimensional antiferromagnetic ordered phase.

I. INTRODUCTION

Metal graphites have received considerable attention partly because of physical and chemical properties related to the low dimensional nature of metal atoms encapsulated in the interlamellar space between graphite layers.[1–7] A metal graphite has a unique layered structure. Ideally, metal atoms (such as V, Cr, Mn, Fe, Co, Ni, Cu, Mo, Pd, Ta, and W) form a metal monolayer sandwiched between adjacent graphite layers. Such sandwich structures are periodically stacked along the *c* axis perpendicular to the graphite layer. In reality, the observed bodies are likely to consist of metal multilayers, but not a single layer, since sample preparation of the metal graphite is carried out at high temperatures where surface diffusion becomes significant. Each metal layer is formed of nanoparticles in the form of either a one-dimensional (1D) chain or two-dimensional (2D) platelets.[4,5] Unlike graphite intercalation compounds (GIC's) no charge transfer occurs between metal monolayers and graphite layers. The interplanar interaction between metal and graphite layers in metal graphite is considered to be of the van der Waals type and is much weaker than that in GIC's because of the absence of attractive Coulomb interactions.

Pristine Pd metal has a face-centered-cubic (fcc) structure with a lattice constant $(a=3.8898\,\text{Å})$. It has an almost filled narrow *d* band and a partly filled *s* band, which can be designated formally as $(4d)^{10-\xi}(5s)^{\xi}$ $(\xi\approx0)$. Pd has the largest Pauli susceptibility with a Stoner factor $(s=9.37)$.[8] This enhancement brings Pd metal close to a ferromagnetic instability. However, Pd is still paramagnetic because the Stoner criterion for the occurrence of ferromagnetism is not satisfied. This means that the Fermi energy of Pd is not situated at an energy where the density of states has a peak. Such a situation may change in Pd graphite (Pd-*G*) where Pd atoms form multilayers in the limited space. Theoretically Bouarab *et al.*[9] have studied how the positional relation between the peak energy in the density of states and the Fermi energy changes with the number of Pd metal layers. They have predicted that the system is ferromagnetic for two to five layers, and is paramagnetic for systems with a monolayer or more than five layers. Thus it is expected that Pd-*G* may exhibit a quasi-2D ferromagnetic behavior.

In this paper we report our experimental dc and ac magnetic susceptibility results of Pd-*G* based on natural graphite (NG) using a superconducting quantum interference device (SQUID) magnetometer. The static and dynamic properties of spin fluctuations are extensively studied. We show that Pd-*G* shows magnetic phase transitions around either 3.8 K [for convenience this sample is denoted as Pd-$G(1)$] or 14 K [Pd-$G(2)$], depending on the sample. An irreversible effect of magnetization is observed, suggesting the frustrated nature of granular systems. The magnetic properties of Pd-$G(2)$ will be discussed in comparison with those of stage-2 $NiCl_2$ GIC,[10] where the ferromagnetic layers are antiferromagnetically stacked along the *c* axis. Here we note that the SQUID dc magnetization of Pd-$G(2)$ was already measured by Mendoza *et al.*[1] The zero-field-cooled magnetization (M_{ZFC}) at an external magnetic field H (= 10 Oe) shows a small peak around 14 K in addition to a broad maximum above 50 K which is typically observed in pristine Pd metal.

II. BACKGROUND: STRUCTURE OF Pd-*G*

$PdCl_2$ GIC belongs to an acceptor type GIC, where charge transfer occurs from graphite layer to intercalate layer.[11] In the Raman spectra of $PdCl_2$ GIC the graphite signal is shifted up in wave number relative to that of pristine graphite.[6] The synthesis of Pd-*G* can be made from the reduction of $PdCl_2$ GIC as a precursor material. The reduction can be carried out (i) in liquid Li diphenlide at room temperature[6] or (ii) in the gaseous phase by contact with hydrogen gas at high temperature (350–400 °C).[5,7] The structural properties of Pd-*G* are different for these two methods of reduction. In Pd-*G* pre-

pared by method (i), there is charge transfer between C and Pd.[6] In fact, the Raman spectrum is similar but not identical to that of $PdCl_2$ GIC precursor. The Pd nanoparticles form mainly monolayers. The size of the Pd nanoparticles is relatively small. The in-plane structure of Pd nanoparticles is commensurate with the graphite lattice, forming a $p(3\times3)$ superlattice.[6]

In Pd-G prepared by method (ii),[7] Pd nanoparticles form mainly multilayer systems with an average thickness of trilayers. The size of Pd nanoparticles is larger than that of Pd nanoparticles prepared by method (i). The Raman spectrum is similar to that of graphite, suggesting that no charge transfer occurs between C and Pd. The in-plane structure of nanoparticles is almost commensurate with that of the graphite host, forming either a $p(2\times2)$ or a $p(3\times3)$ within a mismatch of $\approx$4% in lattice constant.[7] Note that such a mismatch of $\approx$4% is quite often observed between bulk material and nanoparticles of the same material.

III. EXPERIMENTAL PROCEDURE

In the present work we used two kinds of Pd-G samples [denoted as Pd-$G(1)$ and Pd-$G(2)$]. Both samples were prepared from hydrogen reduction of $PdCl_2$ GIC based on natural graphite flakes (grade: RFL 99.9 S) from Kropfmuhl, Germany. Pd-$G(1)$ was reduced for 2 h at 350 °C and Pd-$G(2)$ for 2 days at 400 °C. The structure was studied by transmission electron microscope (TEM)/selected area electron diffraction (SAED) for Pd-$G(1)$ and Pd-$G(2)$ and additionally by x-ray photoelectron spectroscopy (XPS) for Pd-$G(2)$. Bright field transmission electron microscope (TEM) images showed encapsulated nanoparticles. The corresponding SAED pattern from areas occupied by particles and empty regions showed that the reduction was complete. No reflections from the $PdCl_2$ GIC precursor could be obtained. On the other hand all SAED patterns showed reflections from carbon and additional reflections from palladium, if nanoparticles were examined. These Pd particles showed hexagonal and hcp reflections[6,7] which are quite distinguishable from the common fcc Pd. Commensurate superstructures to graphite were observed.[6,7] A comparison of XPS core level spectra from $PdCl_2$ GIC precursor and Pd-G showed that the reduction was complete. Diffraction pattern as well as the XPS signal gave no hint for Pd-hydride formation. The majority of the Pd particles had oval shapes. Their sizes ranged (measured on the long axis of the oval shaped particles) from 20 to 2000 Å. The average size was 530 ± 340 Å. Nanoparticles remain immobile because of their relatively large sizes and high masses. They are not able to diffuse from the carbon lattice. So far no determination has been made for the composition of Pd-G samples. The stoichiometry of stage-3 $PdCl_2$ GIC as a starting material is known as $C_{14.8}PdCl_2$.[12] If only Cl atoms leave as HCl during the reduction, the composition of Pd-G is considered to be described by C_nPd with $n=14.8$. The dc magnetization and ac magnetic susceptibility of Pd-G were measured using a SQUID magnetometer (Quantum Design, MPMS XL-5) with an ultra-low-field capability option.

(i) *SQUID dc magnetization*. Before setting up a sample at 298 K, a remanent magnetic field in the superconducting magnet was reduced to less than 3 mOe using an ultra-low-field capability option. For convenience, hereafter this remanent field is noted as the state $H=0$. The sample was cooled from 298 to 1.9 K at $H=0$. After an external magnetic field (H) was applied at 1.9 K, the zero-field-cooled magnetization (M_{ZFC}) was measured with increasing T from 1.9 to 298 K. Subsequently, the field-cooled magnetization (M_{FC}) was measured with decreasing T from 298 to 1.9 K in the presence of the same H. After the measurement of M_{ZFC} and M_{FC} at H were completed, a series of measurements of M_{FC} were carried out at higher H in the following way. The sample was heated from 1.9 to 298 K. The magnetic field H was changed at 298 K. Then M_{FC} was measured with decreasing T from 298 to 1.9 K in the presence of H.

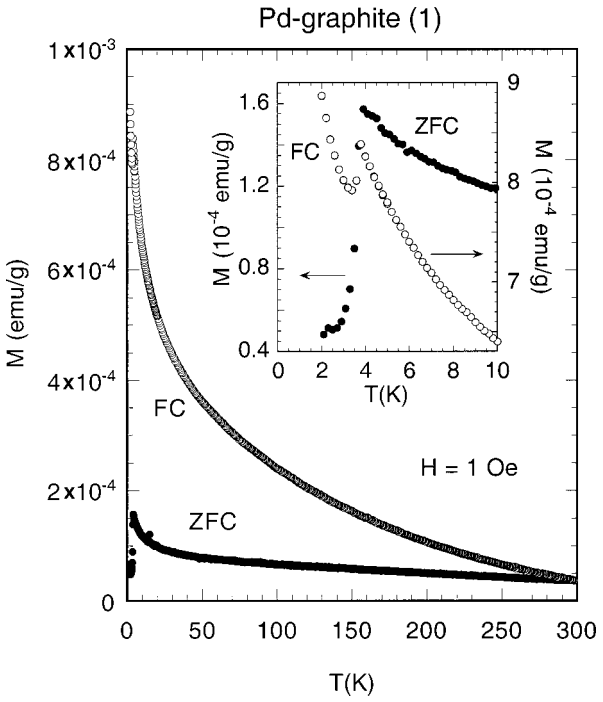

FIG. 1. T dependence of M_{ZFC} (●) and M_{FC} (○) for Pd-$G(1)$. $H=1$ Oe.

(ii) *SQUID ac magnetic susceptibility* ($\chi=\chi'+i\chi''$). A sample was cooled from 298 to 1.9 K at $H=0$. Then both χ' and χ'' were simultaneously measured with increasing T from 1.9 K to high temperature T_h in the absence and presence of H, where the frequency and amplitude of the ac magnetic field were $f=0.07$ Hz–1 kHz and $h=1-2$ Oe, respectively. After each T scan the magnetic field H was changed at high temperature T_h. The sample was cooled from T_h to 1.9 K. Then the measurement was repeated with increasing T from 1.9 K to T_h in the presence of H.

IV. RESULT

A. Pd-$G(1)$

The sample used in the present work consists of many flakes whose c axis are assumed to be randomly aligned over all directions. Figure 1 shows the T dependence of M_{ZFC} and M_{FC} for Pd-$G(1)$ at $H=1$ Oe. The deviation of M_{ZFC} from M_{FC} starts to appear below 298 K, showing a behavior reminiscent of spin glasses. M_{ZFC} shows a sharp peak around 3.8

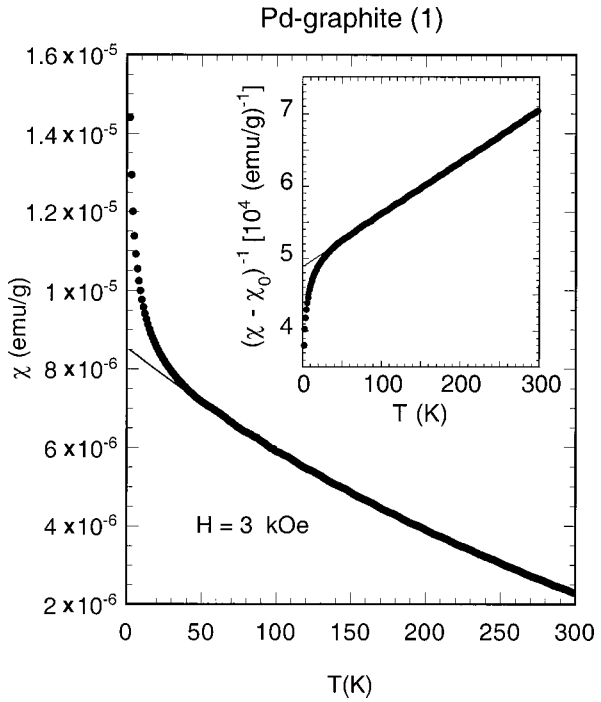

FIG. 2. T dependence of $\chi_{\mathrm{FC}}(=M_{\mathrm{FC}}/H)$ for Pd-$G(1)$. $H=3$ kOe. The inset shows the T dependence of the reciprocal susceptibility, where the straight line is denoted by Eq. (1) with parameters given in the text.

K, while M_{FC} shows a peak around 3.9 K (see the inset). Figure 2 shows the T dependence of $\chi_{\mathrm{FC}}(=M_{\mathrm{FC}}/H)$ for Pd-$G(1)$ at $H=3$ kOe. The susceptibility χ_{FC} obeys a Curie-Weiss law over a wide temperature range ($40\leqslant T\leqslant 298$ K). The least-squares fit of the data to the Curie-Weiss form

$$\chi_g=\frac{C_g}{T-\Theta}+\chi_g^0 \tag{1}$$

yields $C_g=(1.389\pm 0.020)\times 10^{-2}$ emu K/g, $\Theta=-679.2\pm 6.0$ K, and $\chi_g^0=(-1.189\pm 0.012)\times 10^{-5}$ emu/g, where Θ is the Curie-Weiss temperature, C_g is the Curie-Weiss constant, and χ_g^0 is the temperature-independent susceptibility. The inset of Fig. 2 shows the reciprocal susceptibility defined by $(\chi_g-\chi_g^0)^{-1}$ as a function of T. The data are well fitted with a straight line described by Eq. (1). The negative sign of Θ indicates that the interaction between Pd atoms is antiferromagnetic. The susceptibility χ_g^0 is negative, reflecting the nature of diamagnetic susceptibility arising from graphite layers. If the magnetic moment is assigned to every Pd atom and the composition is given by $C_{14.8}Pd$ for Pd-$G(1)$, the effective magnetic moment P_{eff} can be estimated as $P_{\mathrm{eff}}=5.62\pm 0.04\mu_B$. For further discussion, in Sec. V A we define the effective magnetic moment per Pd atom, p_c, which is related to P_{eff} through the relation $P_{\mathrm{eff}}^2=p_c(p_c+2)$: $p_c=4.71\mu_B$. What is the saturation magnetization M_s? Since we have no data of M vs T at H above 3 kOe, the value of M_s cannot be exactly determined experimentally. In spite of that, we assume that M_s is roughly equal to the value of M_{FC} at 2 K for $H=3$ kOe. Then we have $M_s=4.32\times 10^{-2}$ emu/g$=12.29$ emu/Pd mol if the composition $C_{14.8}Pd$ is assumed. The saturation magnetic moment per Pd atom

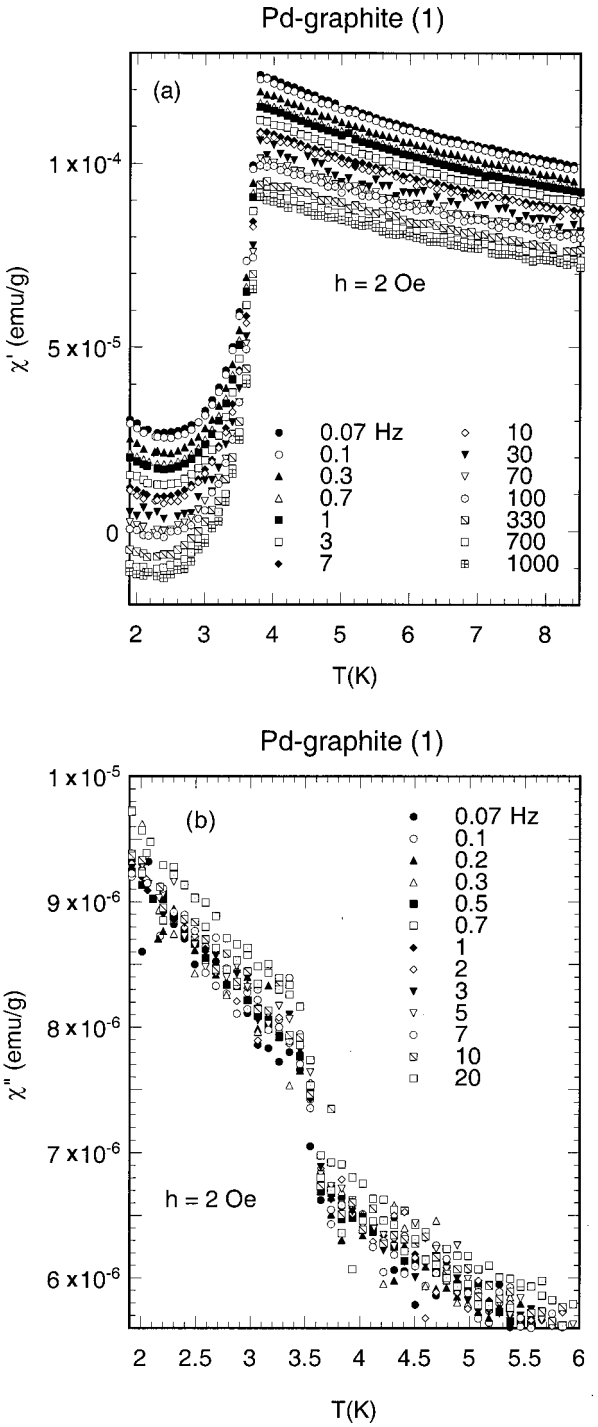

FIG. 3. T dependence of (a) χ' and (b) χ'' for Pd-$G(1)$ at various f. $H=0$ Oe. $h=2$ Oe.

$p_s(=M_s/N_A\mu_B)$ can be estimated as $p_s=2.2\times 10^{-3}\mu_B$. This value of p_s is much smaller than that of p_c. The ratio p_c/p_s is 2141. Note that this ratio is independent of the composition and mass used in the calculation.

Figure 3(a) shows the T dependence of χ' for Pd-$G(1)$ at various f in the absence of H. The amplitude of the ac field is $h=2$ Oe. The dispersion χ' shows a sharp peak at T_N ($=3.8$ K). This peak temperature is independent of f for $0.07\leqslant f\leqslant 1000$ Hz, suggesting that no spin-glass-like behavior occurs around T_N in spite of the irreversible effect of magnetization below 298 K (Fig. 1). In contrast, the value of

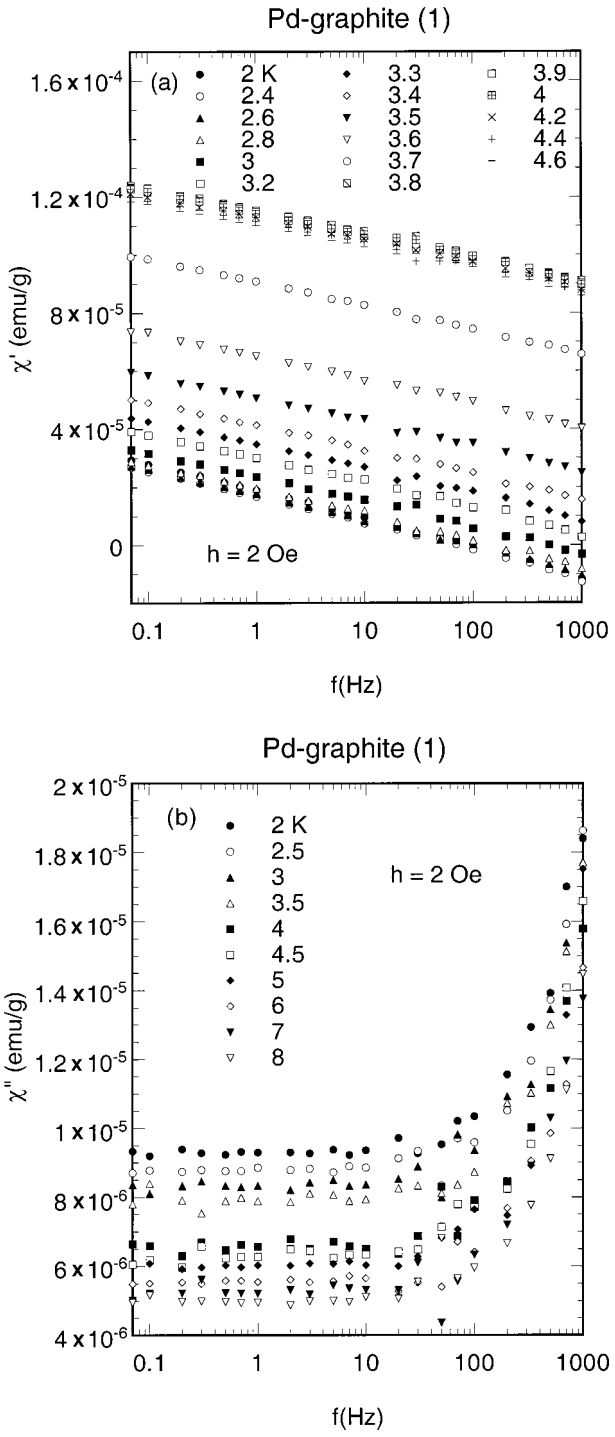

FIG. 4. f dependence of (a) χ' and (b) χ'' for Pd-$G(1)$ at various T. $h=2$ Oe. $H=0$ Oe.

χ' is strongly dependent on f, reflecting the nature of disordered spin system. In the presence of an external magnetic field H, the peak of χ' shifts to the low-temperature side with increasing H (3.3 K at $H=140$ Oe), indicating the antiferromagnetic phase below T_N. Figure 3(b) shows the T dependence of χ'' for Pd-$G(1)$. A drastic decrease of χ'' with increasing T is observed near 3.5 K just below T_N.

Figure 4(a) shows the f dependence of χ' for Pd-$G(1)$ at various T. The dispersion χ' decreases with increasing f. Figure 4(b) shows the f dependence of χ'' for Pd-$G(1)$ at various T. For any T between 2 and 8 K, χ'' is almost independent of f below 10 Hz but drastically increases with increasing f above 10 Hz. Here we assume that χ'' is described by a Debye-type relaxation with a single characteristic relaxation time τ given by

$$\chi'' \approx \frac{\omega\tau}{1+(\omega\tau)^2}, \tag{2}$$

which has a peak at $\omega\tau=1$. Our data suggest that the peak may exist for $f>1000$ Hz for any T between 2 and 8 K, implying that the relaxation time τ is at least shorter than 1.6×10^{-4} sec.

B. Pd-$G(2)$

Figures 5(a) and (b) show the T dependence of M_{ZFC} and M_{FC} for Pd-$G(2)$ at $H=1$ Oe. The magnetization M_{ZFC} shows a broad peak around 52 K and a sharp peak at 14 K. The deviation of M_{ZFC} from M_{FC} starts to appear below 298 K, showing a behavior reminiscent of spin glasses. This behavior may be due partly to spin frustration effects arising from competing interactions among nanoparticles: spins may be partially ordered within nanoparticles even at 298 K. The magnetization M_{FC} dramatically increases with decreasing T below 14–15 K. The T dependence of M_{FC} can be well described by a power-law form given by

$$M_{\mathrm{FC}}=A[(T_0-T)/T_0]^{\beta}+B, \tag{3}$$

for $9\leqslant T\leqslant 14.4$ K, where $T_0=14.81\pm0.05$ K, $\beta=0.367\pm0.009$, $A=0.0298\pm0.0002$ (emu/g), and $B=0.0791\pm0.0004$ (emu/g). The critical exponent β of magnetization thus obtained is close to that predicted for 3D spin systems: $\beta=0.31$ for Ising symmetry, $\beta=0.33$ for XY symmetry, and $\beta=0.35$ for Heisenberg symmetry.[13] This result suggests that a 3D long-range spin order may develop below T_0.

Figure 6 shows the T dependence of χ_{FC} for Pd-$G(2)$ at $H=3$ kOe. The measurement was done with increasing T in the presence of H. The susceptibility χ_{FC} obeys a Curie-Weiss behavior in the limited temperature range ($100\leqslant T\leqslant 270$ K). The least-squares fit of these data χ vs T to Eq. (1) yields $C_g=(5.0041\pm0.098)\times10^{-2}$ emu K/g, $\Theta=25.42\pm1.25$ K, and $\chi_g^0=(-1.431\pm0.035)\times10^{-4}$ emu/g. The inset of Fig. 6 shows the reciprocal susceptibility defined by $(\chi_g-\chi_g^0)^{-1}$ as a function of T. The data are well fitted with a straight line described by Eq. (1) within the limited temperature range. The positive sign of Θ suggests that the intraplanar exchange interactions between Pd atoms may be ferromagnetic. Since $T_0=14.81$ K and $\Theta=25.42$ K, the ratio T_0/Θ is estimated as 0.58, which is much smaller than 1 as predicted by the molecular-field theory. This result suggests that the system magnetically behaves like a quasi-2D spin system. Here we assume that Pd nanoparticles act as localized spins and the effective magnetic moment is assigned to every Pd atom. If the composition of Pd-$G(2)$ is given by $C_{14.8}Pd$, the effective magnetic moment P_{eff} can be estimated as $P_{\mathrm{eff}}=10.76\pm0.08\mu_B$. Correspondingly, another effective magnetic moment p_c per Pd atom is given by $p_c=9.81\mu_B$.

Figure 7 shows the H dependence of M_{FC} for Pd-$G(2)$ at various T. The magnetization drastically changes around a characteristic field $H_a^0\approx200$ Oe, reflecting a transition from the antiferromagnetic state to the ferromagnetic state. Similar

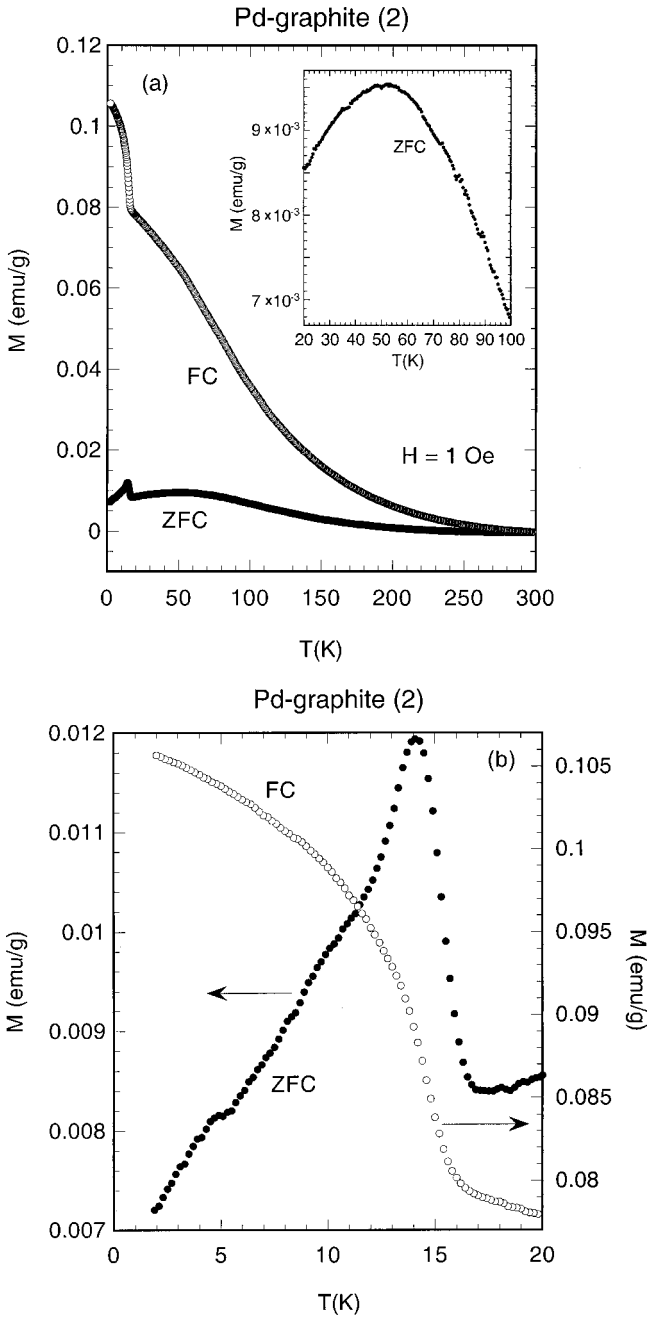

FIG. 5. (a) and (b) T dependence of M_{ZFC} (●) and M_{FC} (○) for Pd-$G(2)$. $H=1$ Oe.

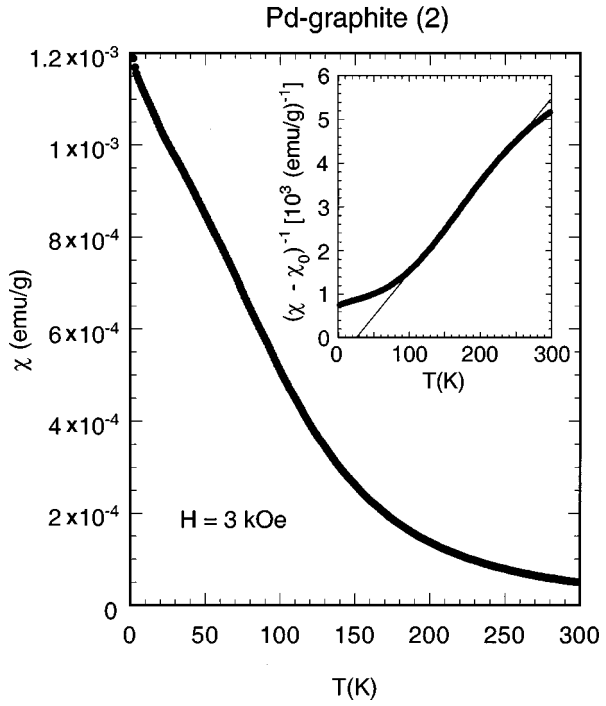

FIG. 6. T dependence of χ_{FC} at $H=3$ kOe for Pd-$G(2)$. The inset shows the T dependence of the reciprocal susceptibility, where the straight line is denoted by Eq. (1) with parameters given in the text.

behavior is also observed in stage-2 $NiCl_2$ GIC.[10] Here we note that Fig. 7 is derived from the data of M_{FC} vs T for various H, but not the data obtained directly from the measurement of M_{FC} vs H with increasing H for each T. What is the saturation magnetization M_s in Pd-$G(2)$? From Fig. 7 the saturation magnetization M_s is roughly estimated as $M_s=5$ emu/g or 1421 emu/Pd mol at $H=40$ kOe when the composition of $C_{14.8}Pd$ is assumed. If the saturation magnetization is assigned to every Pd atoms, the saturation magnetic moment per Pd atom $p_s(=M_s/N_{A\mu B})$ can be estimated as $p_s=0.25\mu_B$. This value of p_s is very different from that of p_c. The ratio p_c/p_s is 39.2.

Figures 8(a) and (b) show the T dependence of χ' and χ'' for Pd-$G(2)$ at various f, where $h=1$ Oe. The dispersion χ' exhibits a peak at 14.3 K and a small shoulder around 11 K. The T dependence of χ' in Pd-$G(2)$ is similar to that of stage-2 $NiCl_2$ GIC.[17] The peak temperature (=14.3 K) is

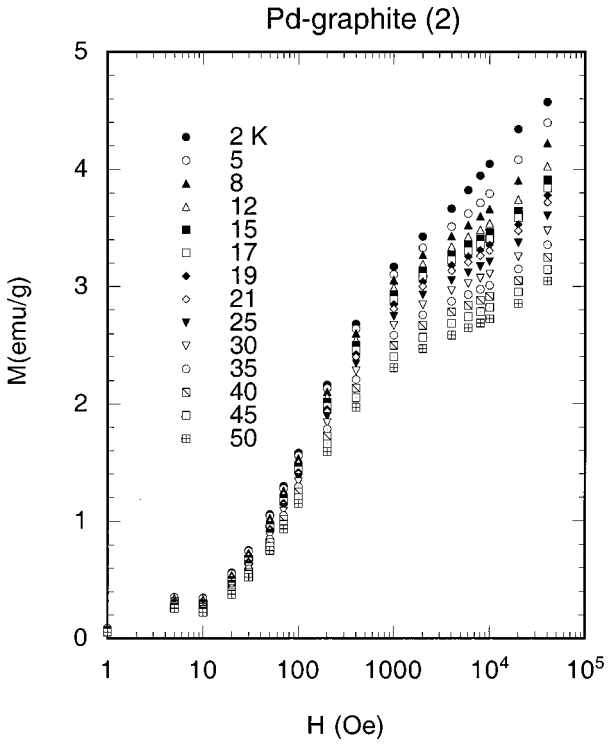

FIG. 7. H dependence of M_{FC} at various T for Pd-$G(2)$.

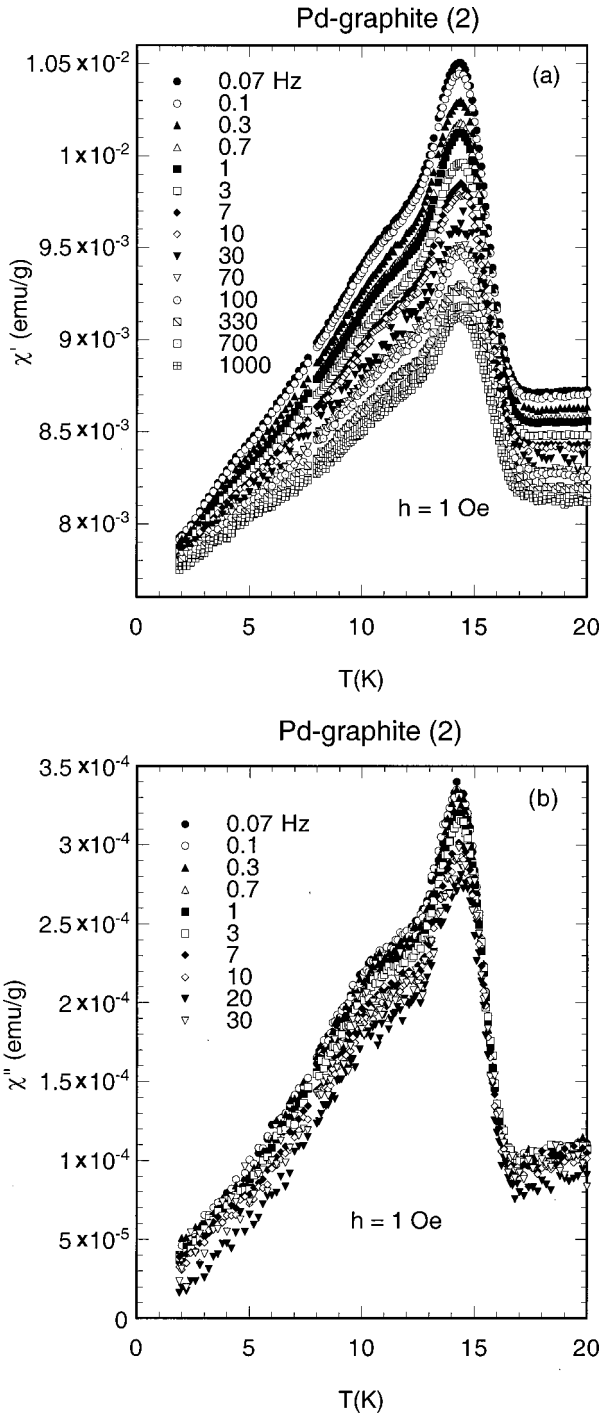

FIG. 8. T dependence of (a) χ' and (b) χ'' for Pd-$G(2)$ at various f. $H=0$ Oe. $h=1$ Oe.

independent of f for $0.07 \leqslant f \leqslant 1000$ Hz. In contrast, the value of χ' drastically decreases with increasing f at the same T, reflecting the nature of disordered spin systems. The absorption χ'' also shows a sharp peak at $T_{cu}(=14.2\,\mathrm{K})$ and a small shoulder around $T_{cl}(=11\,\mathrm{K})$. The peak temperature of χ'' is almost independent of f for $0.07 \leqslant f \leqslant 1000$ Hz, suggesting that no spin-glass-like behavior occurs around T_{cu} in spite of the irreversible effect of magnetization below 298 K [Fig. 5(a)].

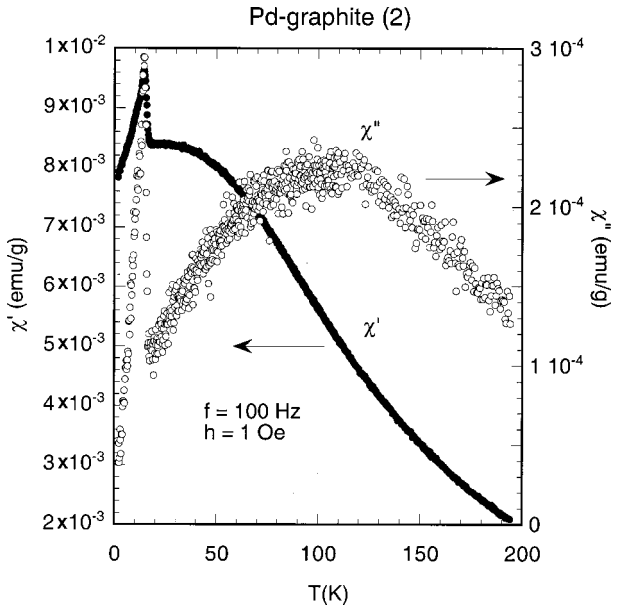

FIG. 9. T dependence of (a) χ' and (b) χ'' for Pd-$G(2)$. $H=0$ Oe. $f=100$ Hz. $h=1$ Oe.

Figure 9 shows the T dependence of χ' and χ'' for Pd-$G(2)$ in the absence of H, where $f=100$ Hz and $h=1$ Oe. The data are taken with increasing T. Both χ' and χ'' exhibit a peak around 14 K. Above this temperature χ'' exhibits a very broad peak around 100 K. Note that M_{ZFC} at $H=1$ Oe for Pd-$G(2)$ has a broad peak around 52 K [see the inset of Fig. 5(a)], while the dc magnetic susceptibility of pristine Pd has a very broad peak around 85 K.[8]

Figures 10(a) and (b) show the T dependence of χ' and χ'' for Pd-$G(2)$ in the presence of H, respectively, where $h=1$ Oe and $f=100$ Hz. The peak of χ' slightly shifts to the higher temperature side with increasing H: 14.3 K at $H=0$ and 14.85 K at $H=70$ Oe. This peak disappears above 70 Oe. This implies that the in-plane ferromagnetic order is apparently enhanced by the application of H. In contrast, the peak of χ'' shifts to the low-temperature side with increasing H: 14.3 K at $H=0$ and 13.19 K at $H=5$ Oe. The peak disappears above 10 Oe, suggesting that the anisotropy field in the c plane, H_A^{in}, is on the order of 5 Oe.

Figure 11(a) shows the f dependence of χ' for Pd-$G(2)$ at various T. It is found that χ' can be well described by a power-law form ($\chi' \approx \omega^{-x}$) over the whole frequency range used in the present work. Figure 11(b) shows the T dependence of x for Pd-$G(2)$, which is similar to the T dependence of χ'' at $H=0$ [see Fig. 8(b)]. The exponent x is positive and very close to zero, and exhibits a local maximum around T_{cu} as well as a broad shoulder around T_{cl}. Similar behavior is observed in stage-2 $NiCl_2$ GIC,[10] where the value of x takes a local maximum at 16.5 K just below T_{cl} $(=17.2\,\mathrm{K})$ and at 21.1 K just above $T_{cu}(=20.5\,\mathrm{K})$.

Figure 12 shows the f dependence of χ'' for Pd-$G(2)$ at various T. The f dependence of χ'' for $f<20$ Hz is rather different from that for $f \geqslant 20$ Hz depending on T. Below 17 K the absorption χ'' decreases with increasing f for $f<20$ Hz,

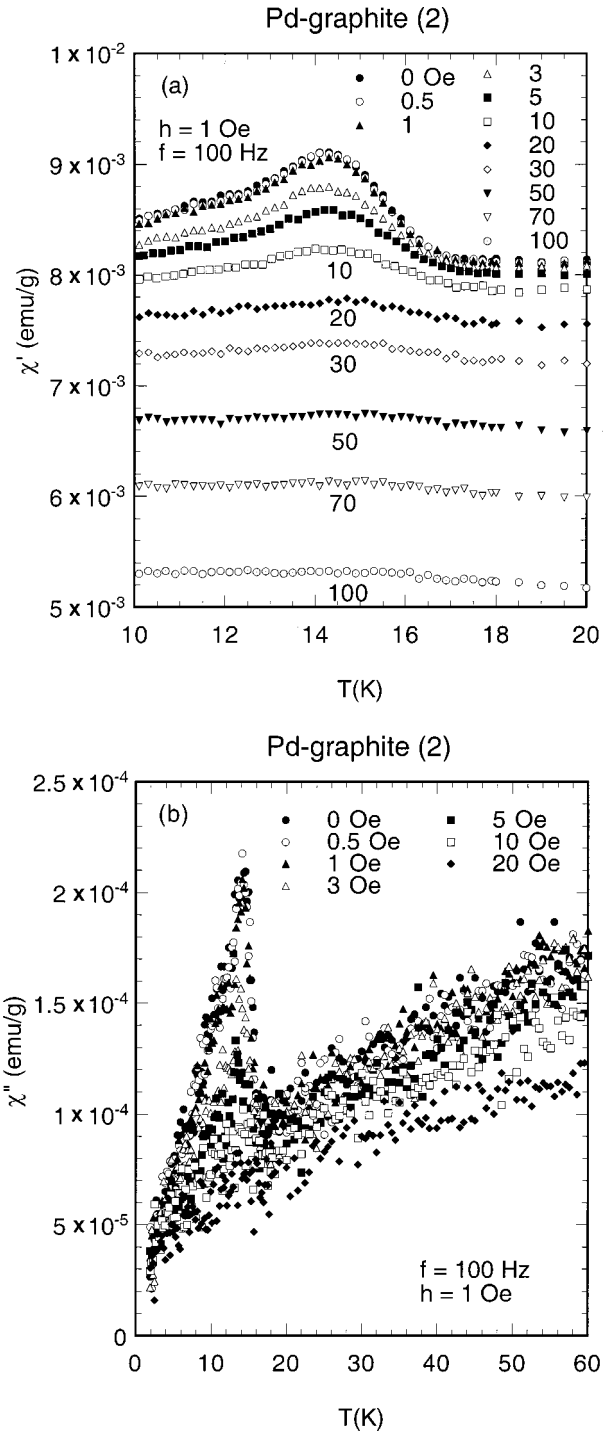

FIG. 10. T dependence of (a) χ' and (b) χ'' for Pd-$G(2)$ at various H. $f=100$ Hz. $h=1$ Oe.

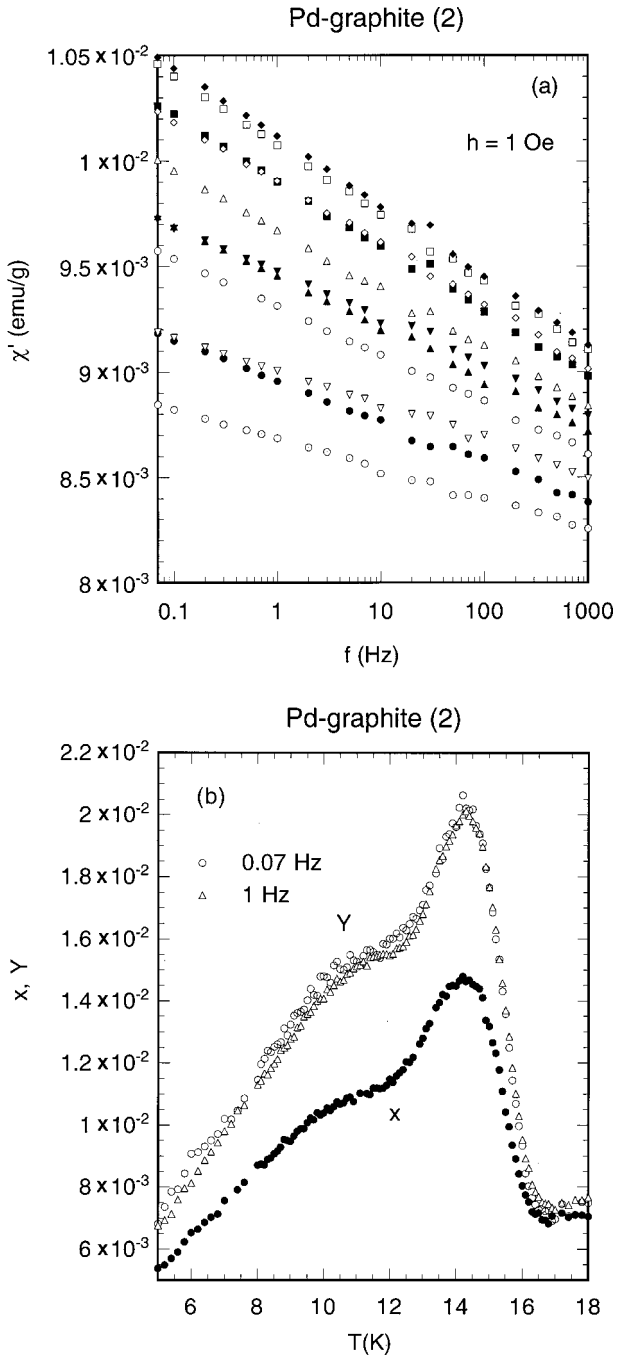

FIG. 11. (a) f dependence of χ' for Pd-$G(2)$ at various T. $h=1$ Oe. $T=9$ (●), 11 (○), 12 (▲), 13 (△), 13.5 (■), 14 (□), 14.5 (◆), 15 (◇), 15.5 (▼), 16 (▽), and 16.5 K (⊙). (b) T dependence of exponent x ($\chi' \approx \omega^{-x}$) (●) and $Y[=(2/\pi)(\chi''/\chi')]$ at $f=0.07$ Hz (○) and 1 Hz (△).

while it increases with increasing f for $f>20$ Hz. Note that such behavior is also observed in stage-2 $NiCl_2$ GIC.[10]

V. DISCUSSION

A. Itinerant spin systems

Before discussion, we summarize the magnetic properties of Pd-$G(1)$ and Pd-$G(2)$. Pd-$G(1)$ shows an antiferromagnetic phase transition at $T_N=3.8$ K. The Curie-Weiss temperature is given by $\Theta=-679.2\pm6.0$ K. The ratio of the magnetic moments p_c/p_s is about 2140. This ratio may be overestimated because the magnetization used in this calculation is not saturated at 3 kOe which is the highest field for the experiment on Pd-$G(1)$. In contrast, Pd-$G(2)$ undergoes two magnetic phase transitions at $T_{cu}(=14.2$ K) and T_{cl} $(=11$ K). The Curie-Weiss temperature is $\Theta=25.42$ ±1.25 K. The intraplanar interaction is strongly ferromagnetic, while the interplanar interaction is weakly antiferromagnetic. The ratio of the magnetic moments p_c/p_s is 39. Such a large ratio of p_c/p_s is a feature common to itinerant

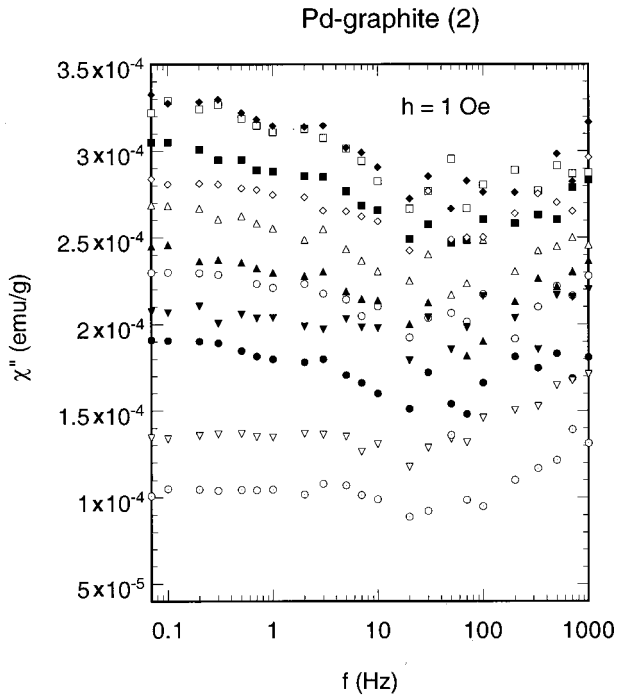

FIG. 12. f dependence of χ'' for Pd-$G(2)$ at various T. $h=1$ Oe. The same notations are used as in Fig. 11(a).

spin systems where the d electrons responsible for magnetism are mobile. According to Moriya,[14] there is some correlation between p_c/p_s vs T_C for ferromagnetic metals, where T_C is the Curie temperature. In the local limit for well-defined localized moment, the ratio p_c/p_s is independent of T_C and is nearly equal to 1. In the opposite weakly ferromagnetic limit, the theory predicts the divergence of this ratio as $p_s \rightarrow 0$ or $T_C \rightarrow 0$, since the Curie-Weiss constant in this case is independent of p_s or T_C. The ratio p_c/p_s is much larger than 1 for small T_C and the ratio is generally close to 1 for very large T_C. The Rhodes-Wohlfarth plot (p_c/p_s vs T_C) (Ref. 15) for various spin systems clearly indicates that the values of p_c/p_s are distributed almost continuously between these two extremes. The spin density fluctuations show various properties ranging between the two opposite extremes: the local moment limit (spin fluctuations localized in real space) and the limit of weakly ferro- and antiferromagnetic metals (spin fluctuations localized in reciprocal space; extended in real space). It has been believed that the Curie-Weiss law is attributed exclusively to the local spin system. However, this law is also observed in the itinerant spin system. In conclusion, Pd-$G(1)$ is an itinerant spin system with mainly antiferromagnetic interactions, while Pd-$G(2)$ is an itinerant spin system with mainly ferromagnetic interactions. We note that the magnetic properties of Pd-G strongly depend on the reaction times required for the hydrogen gas reduction: ferromagnetic nature for the long reaction time [Pd-$G(2)$] and the antiferromagnetic nature for the short reaction time [Pd-$G(1)$]. This result suggests that the magnetic property of Pd-G is closely related to the structure of Pd nanoparticles.

B. Effect of Pd nanoparticles on magnetic susceptibility in Pd-$G(1)$

We discuss the magnitude of the temperature-independent susceptibility $\chi_g^0=(-11.89\pm0.12)\times10^{-6}$ emu/g for Pd-$G(1)$. We assume that χ_g^0 may be described by

$$\chi_g^0=[12.011n\,\chi_g^0(\mathrm{C})+106.4\chi_g^0(\mathrm{Pd})]/(12.011n+106.4), \tag{4}$$

for Pd-G having the composition C_nPd, where χ_g^0(C) and χ_g^0(Pd) are the susceptibility per gram of pristine graphite and Pd, respectively. For $n=14.8$, χ_g^0 can be rewritten as $\chi_g^0=0.626\chi_g^0(\mathrm{C})+0.374\chi_g^0(\mathrm{Pd})$. The susceptibility χ_g^0(C) corresponds to a powder-averaged susceptibility of graphite given by $\chi_g^0(\mathrm{C})=(\frac{2}{3})\chi_g^a+(\frac{1}{3})\chi_g^c$, where χ_g^c along the c axis is diamagnetic and weakly dependent on T. The susceptibility χ_g^a is positive and almost independent of T. Note that the magnitude of χ_g^c is much larger than that of χ_g^a

It is interesting to estimate the value of χ_g^0 as a function of T using the data of pristine graphite (highly oriented pyrolytic graphite, HOPG) (Ref. 16) and pristine Pd. The data of pristine Pd is obtained by van Leeuwen *et al.*[8] The calculated value of χ_g^0 is dependent on T. It decreases with decreasing T: -1.69×10^{-6} emu/g at 290 K to -2.38×10^{-6} emu/g at 100 K. These values are relatively larger than the experimental value of $\chi_g^0(=-11.89\times10^{-6}$ emu/g) for Pd-$G(1)$. What is the cause of this discrepancy? One possibility is that the diamagnetic susceptibility of graphite χ_g^0(C) may be described by χ_g^c because samples are formed of small flakes which may be rather different from ideal powders: $\chi_g^0(\mathrm{C})=\chi_g^c$. When the formula $\chi_g^0=0.626\chi_g^c+0.374\chi_g^0(\mathrm{Pd})$ is used, we find that the calculated value of χ_g^0 decreases with decreasing T: -9.734×10^{-6} emu/g at 290 K to -13.420×10^{-6} emu/g at 100 K. These values are close to the experimental result. A second possibility is that the susceptibility from Pd may decrease with decreasing size of nanoparticles. In fact, in Pd clusters/colloids with diameters ranging from 25–150 Å, van Leeuwen *et al.*[8] have observed a dramatic reduction of the susceptibility with particle size.

C. Nature of spin ordering in Pd-$G(2)$

Pd-$G(2)$ approximates a quasi-two-dimensional (2D) XY-like ferromagnet with an extremely weak antiferromagnetic interplanar exchange interaction, in spite of the character of itinerant spin systems. The effective spin Hamiltonian of Pd-$G(2)$ may be described by

$$\mathcal{H}=-2J\sum_{\langle i,j\rangle}\mathbf{S}_i\cdot\mathbf{S}_i+D\sum_i(S_i^z)^2-2J'\sum_{\langle i,m\rangle}\mathbf{S}_i\cdot\mathbf{S}_m, \tag{5}$$

where $\hbar\mathbf{S}$ is the effective spin angular momentum, the z axis coincides with the c axis, J (>0) is the ferromagnetic intraplanar interaction, $D(>0)$ is the single ion anisotropy term, and $J'(<0)$ is the antiferromagnetic interplanar interaction. For convenience the equivalent interaction fields at 0 K are defined as $H_A^{\mathrm{out}}=DS/g_c\mu_B$, $H_{E'}=2z'|J'|S/g_a\mu_B$, $H_E=2zJS/g_a\mu_B$, and $H_{SF}=[2H_A^{\mathrm{in}}H_{E'}]^{1/2}$ where g_a and g_c are the g values along the c plane and c axis ($g_a=g_c=2$ is

assumed). H_E is the intraplanar exchange field, $H_{E'}$ the interplanar exchange field, H_{SF} the spin flop field, H_A^{in} the anisotropy field in the c plane, H_A^{out} the anisotropy field along the c axis, and z and z' the numbers of interacting neighbors in and between the c plane, respectively ($z=z'=6$). The value of S is estimated as 4.9 from the relation $P_{eff}=g[S(S+1)]^{1/2}$ with $P_{eff}=10.76\pm0.08\mu_B$. The value of J is calculated to be $J=0.22\pm0.01$ K from the relation $\Theta=2zJS(S+1)/3k_B$. The value of $H_{E'}$ is estimated as $H_{E'}=H_a^0/2=100$ Oe (see Ref. 10 for this relation) using the value of H_a^0 derived from Fig. 7. The value of H_A^{in} is also estimated as $H_A^{in}\approx5$ Oe from Fig. 10(b), leading to $H_{SF}\approx30$ Oe. Then the value of $|J'|$ is on the order of 2.8×10^{-4} K, which is much weaker than the intraplanar interaction: $|J'|/J\approx1.3\times10^{-3}$.

What is the mechanism of two magnetic phase transitions at T_{cu} and T_{cl} in Pd-$G(2)$? The Pd layers of this compound are formed of Pd nanoparticles. This finite size of nanoparticles is a crucial element in the magnetic phase transition of this compound. The effective interplanar exchange interaction J'_{eff} between spins over the in-plane spin correlation length ξ in adjacent Pd layers is described by $J'_{eff}=J'(\xi/a)^2$, where J' is the interplanar exchange interaction and a is the in-plane lattice constant. The growth of ξ is limited by island size as T is decreased. Suppression of the increase in J'_{eff} leads to the realization of 2D spin ordering between T_{cu} and T_{cl}. Below T_{cl} there occurs a 3D spin ordering where the 2D ferromagnetic layers are antiferromagnetically stacked along the c axis. Note that similar behavior is observed in stage-2 $NiCl_2$ GIC with $T_{cu}(=20.5\pm0.2\,K)$ and $T_{cl}(=17.2\,K)$.[10]

D. Origin of magnetic interaction

It is well known that pristine Pd is close to ferromagnetism, but not a ferromagnet. The enhanced susceptibility of pristine Pd is described by $\chi_g(\mathrm{Pd})=s\chi_g^0(\mathrm{Pd})$ with $\chi_g^0(\mathrm{Pd})=2\mu_B^2N_d(E_F)$, where s is a Stoner factor ($s=9.37$) and $N_d(E_F)$ is the density of states for d-band electrons per spin at the Fermi level E_F. The value of s is much larger than that of other metals. What is the origin of the intraplanar ferromagnetic interaction in Pd-$G(2)$? This ferromagnetic nature is considered to be related to the Stoner condition of ferromagnetism. When U is the Coulomb interaction between d electrons belonging to the same atom, the ferromagnetic state can exist at $T=0$ K only for $U>U_{cr}$, where $U_{cr}=1/N_d(E_F)$. Ferromagnetism is more favorable as U_{cr} becomes as small as possible. This means that Fermi energy should be located at a maximum of the density of states.

The origin of the interplanar antiferromagnetic exchange interaction may be similar to that of $CoCl_2$ GIC. According to Yeh *et al.*,[17] the dominant interplanar exchange interaction in stage-1 $CoCl_2$ GIC is the superexchange interaction, while both the dipole-dipole interaction and superexchange interaction are equally important in stage-2 $CoCl_2$ GIC. For higher stage $CoCl_2$ GIC, the dipole-dipole interaction dominates because of the rapid decrease of the superexchange interaction with increasing stage number. For the large separation distance the interplanar exchange interaction may be described by the dipole-dipole interaction between $\mathbf{S}_i$ and $\mathbf{S}_m$,

$$H_{d-d}=(g_a\mu_B)^2\left(\frac{\mathbf{S}_i\cdot\mathbf{S}_m}{R_{im}^3}-\frac{3(\mathbf{S}_i\cdot\mathbf{R}_{im})(\mathbf{S}_m\cdot\mathbf{R}_{im})}{R_{im}^5}\right). \quad (6)$$

If we assume that the direction of spin $\mathbf{S}_i$ is perpendicular to $\mathbf{R}_{im}$ (or perpendicular to the c axis), then the Hamiltonian $H_{d\text{-}d}$ can be approximated as a form of $2J_{d\text{-}d}(\mathbf{S}_i\cdot\mathbf{S}_m)$ where $J_{d\text{-}d}=(g_a\mu_B)^2/2(R_{im})^3$ is positive and favors the antiferromagnetic interplanar interaction. The value of $J_{d\text{-}d}$ is calculated as $1.246d^{-3}$ [K]$=3.0\times10^{-4}$ K, where $g_a=2$ is assumed and d is the c axis repeat distance in units of Å: $d=16.6$ Å for stage-3 $PdCl_2$ GIC.[11] This value of $J_{d\text{-}d}$ is in good agreement with the value of $|J'|(=2.8\times10^{-4}\,K)$ derived above.

E. Nature of dynamic spin fluctuations in Pd-$G(2)$

We have shown that the power-law form ($\chi'\approx\omega^{-x}$) is valid over the whole frequency range at any T in Pd-$G(2)$. Then χ'' can be calculated as[10,18]

$$\chi''(\omega)=\frac{\pi x}{2}\chi'(\omega)\mathrm{sgn}(\omega), \quad (7)$$

using the Kramers-Kronig relation

$$\chi''(\omega)=-\frac{1}{\pi}P\int_{-\infty}^{\infty}d\omega'\frac{1}{\omega'-\omega}[\chi'(\omega')-\chi^{\infty}], \quad (8)$$

where the notation [sgn(ω)], which is 1 for $\omega>0$ and -1 for $\omega<0$, is included in Eq. (7) because χ'' should be an odd function of ω, and χ^{∞} is the complex susceptibility at $\omega=\infty$ and is assumed to be zero here. In Fig. 11(b) we also show the T dependence of $Y[=(2/\pi)\chi''/\chi']$ at $f=0.07$ and 1 Hz. Although the value of Y is a little larger than that of x at each T, the T dependence of Y is very similar to that of x. These results are consistent with the prediction from Eq. (7). According to the fluctuation-dissipation theorem, the Fourier spectrum $S(\omega)$ of the time-dependent magnetization fluctuation $\langle M(0)M(t)\rangle$ is related to $\chi''(\omega)$ by

$$S_{aa}(\omega)=\int_{-\infty}^{\infty}\langle M_a(0)M_a(t)\rangle e^{-i\omega t}dt=\frac{2k_BT}{\hbar\omega}\chi''_{aa}(\omega), \quad (9)$$

where t is time and $M(t)$ is the time-dependent magnetization. It is expected from Eq. (7) that χ'' at low frequencies is described by the same power-law form as χ': $\chi''\approx\omega^{-x}$. Thus $S(\omega)$ has the form $\omega^{-(1+x)}$, indicating that $\langle M(0)M(t)\rangle$ varies with t as t^x. In the limit of $x\to0$, $\langle M(0)M(t)\rangle$ has a logarithmic time dependence. As shown in Fig. 5(a) at temperatures below 298 K, the magnetization M_{ZFC} is much smaller than the magnetization M_{FC} corresponding to the magnetization in thermal equilibrium. The magnetization M_{ZFC} may increase and reach M_{FC} with t as $\ln(t)$.

As shown in Fig. 12, χ'' for Pd-$G(2)$ has the characteristic f dependence: χ'' decreases with increasing f for $f\leqslant20$ Hz and then increases with f above 20 Hz. This may be explained in terms of the following model. Around T_{cu} and T_{cl}, the internanoparticle spin correlation is still random within each Pd layer. The magnetization of each Pd nanoparticle will fluctuate and change direction relative to other Pd nanoparticles on a certain characteristic time scale depending on

the nanoparticle size and internanoparticle interaction. There are two kinds of relaxation time associated with intrananoparticle fluctuation (τ_{in}) and internanoparticle fluctuation (τ_{out}). The relaxation time τ_{out} is assumed to be much longer than the relaxation time τ_{in}. Correspondingly the characteristic frequencies f_{in} and f_{out} are defined by $(2\pi\tau_{in})^{-1}$ and $(2\pi\tau_{out})^{-1}$, respectively: $f_{in} \gg f_{out}$. When the relaxation of these fluctuations is of the Debye type, χ'' may be described by[10,18]

$$\chi'' = \chi_{in}(\mathbf{Q}=0)\frac{\omega\tau_{in}}{1+(\omega\tau_{in})^2} + \chi_{out}(\mathbf{Q}=0)\frac{\omega\tau_{out}}{1+(\omega\tau_{out})^2}, \tag{10}$$

where $\chi_{in}(\mathbf{Q})$ and $\chi_{out}(\mathbf{Q})$ are the wave-vector-dependent susceptibilities related to the intrananoparticle and internanoparticle fluctuations, respectively. The absorption χ'' has two peaks at $\omega\tau_{in}=1$ (or $f=f_{in}$) and $\omega\tau_{out}=1$ (or $f=f_{out}$). Our results indicate that (i) f_{out} is lower than 0.07 Hz and that (ii) f_{in} is higher than 1 kHz at least below 17 K. No T dependence of f_{in} and f_{out} is observed.

VI. CONCLUSION

The structure of Pd-G is characterized by multilayered Pd nanoparticles. Different reduction conditions lead to different degrees of developed nanoparticles. The magnetic properties of Pd-G are dependent on the reduction conditions: the antiferromagnetic nature for the short reaction time [Pd-$G(1)$] and ferromagnetic nature for the long reaction time [Pd-$G(2)$]. Pd-$G(1)$ magnetically behaves like a antiferromagnetic itinerant spin system. It undergoes antiferromagnetic phase transition at $T_N(=3.8\,\mathrm{K})$. No spin-glass-like behavior occurs around T_N. Pd-$G(2)$ magnetically behaves like a quasi-2D XY-like ferromagnet with very weak antiferromagnetic interplanar interaction. It undergoes magnetic phase transitions at $T_{cu}(=14.2\pm0.2\,\mathrm{K})$ and $T_{cl}(=11\,\mathrm{K})$. Between T_{cu} and T_{cl} a 2D ferromagnetic spin order is established within each Pd nanoparticle in the Pd layer. The ordered phase below T_{cl} is a 3D antiferromagnetic one. The existence of Pd nanoparticles in a reduced dimension is a key to understanding the uniqueness of spin ordering in Pd-G. To be more conclusive on the nature of nanoparticles, further studies are required using small-angle neutron scattering, x-ray scattering, and so on.

ACKNOWLEDGMENTS

One of the authors (J.W.) is grateful to the Science and Technology Agency (Japan) and the Alexander von Humboldt-Foundation (Germany) for financial support. The work at Binghamton was supported by the Research Foundation of SUNY-Binghamton (Contract No. 240-9807A).

*Email address: suzuki@binghamton.edu
†Present address: Department of Materials Science and Processing, Faculty of Engineering, Osaka University, 2-1, Yamada-oka, Suita, Osaka 565-0871, Japan.

[1] D. Mendoza, F. Morales, R. Escudero, and J. Walter, J. Phys.: Condens. Matter **11**, L317 (1999).
[2] M. E. Vol'pin, Yu. N. Novikov, N. D. Lapkina, V. I. Kasatochkin, Yu. T. Struchkov, M. E. Kasakov, R. A. Stukan, V. A. Povitskij, Yu. S. Karimov, and A. V. Zvarikina, J. Am. Chem. Soc. **97**, 3366 (1975).
[3] A. T. Shuvayev, B. Yu. Helmer, T. A. Lyubeznova, V. L. Kraizman, A. S. Mirmilstein, L. D. Kvacheva, Yu. N. Novikov, and M. E. Volpin, J. Phys. (France) **50**, 1145 (1989).
[4] J. Walter, H. Shioyama, and Y. Sawada, Carbon **37**, 41 (1999).
[5] J. Walter and H. Shioyama, Phys. Lett. A **254**, 65 (1999).
[6] J. Walter, Philos. Mag. Lett. **80**, 257 (2000).
[7] J. Walter, Adv. Mater. **12**, 31 (2000).
[8] D. A. van Leeuwen, J. M. van Ruitenbeek, G. Schmidt, and L. J. de Jongh, Phys. Lett. A **170**, 325 (1992).
[9] S. Bouarab, C. Demangeat, A. Mokrani, and H. Dreyssé, Phys. Lett. A **151**, 103 (1990).
[10] I. S. Suzuki and M. Suzuki, J. Phys.: Condens. Matter **10**, 5399 (1998).
[11] P. Behrens, J. Ehrich, W. Metz, and W. Niemann, Synth. Met. **34**, 199 (1989).
[12] W. Rudolf, Z. Anorg. Allg. Chem. **254**, 319 (1947).
[13] L. J. de Jongh and A. R. Miedema, Adv. Phys. **23**, 1 (1974).
[14] T. Moriya, *Spin Fluctuations in Itinerant Electron Magnetism* (Springer-Verlag, New York, 1985).
[15] P. R. Rhodes and E. P. Wohlfarth, Proc. R. Soc. London **273**, 247 (1963).
[16] M. Suzuki, I. S. Suzuki, and J. Walter (unpublished).
[17] N. C. Yeh, K. Sugihara, M. S. Dresselhaus, and G. Dresselhaus, Phys. Rev. B **40**, 622 (1989).
[18] M. Suzuki and I. S. Suzuki, Phys. Rev. B **58**, 840 (1998).